G-16 GROUND MOTION PREDICTION EQUATIONS FOR THE CENTRAL AND EASTERN NORTH AMERICA

V. Graizer(1)

(1) Seismologist, U. S. Nuclear Regulatory Commission, Washington, DC 20555-0001, Vladimir.Graizer@nrc.gov

Abstract

New ground motion prediction equations (GMPE) G-16 model for the Central and Eastern North America (CENA) is presented. The model is developed following the modular filter based approach introduced by Graizer and Kalkan [1, 2] for active tectonic environment in the Western US (WUS). The G-16 model is based on the Next Generation Attenuation database for the CENA (NGA-East) for the horizontal peak ground acceleration and 5%-damped pseudo spectral acceleration RotD50 component (Goulet et al., [3]). A subset of 5026 data points from this database with moment magnitudes **M**≥3.75 and fault distances R_{rup}≤1000 km was used to constrain the G-16 model. The dataset includes 48 earthquakes from different regions in the CENA not distinguishing between the Mid-Continent and Gulf Coast regions. Mid-Continent data dominate the dataset. In contrast to the active tectonic environment the database for the CENA is not sufficient for creating purely empirical GMPE covering the range of magnitudes and distances required for seismic hazard assessments. Recordings in the NGA-East database are sparse and cover mostly range of **M**<6.0 with limited amount of near-fault recordings. For **M**≥6 the G-16 model was adjusted based on a combination of 1) ratios of amplitudes of earthquakes from the NGA-East and NGA-West databases, 2) average stress-drop ratio between WUS and CENA, and 3) recently performed ground motion simulations. The functional forms of the G-16 GMPEs are derived from filters—each filter represents a particular physical phenomenon affecting the seismic wave radiation from the source. Main changes in the functional forms for the CENA relative to the WUS model (Graizer and Kalkan [4]) are a shift of maximum frequency of the acceleration response spectrum toward higher frequencies and an increase in the response spectrum amplitudes at high frequencies. Site correction was developed based on multiple runs of representative V_{S30} profiles through SHAKE-type equivalent-linear programs using time histories and random vibration theory (RVT) approaches. Site amplification functions are calculated for different V_{S30} relative to hard rock definition used in nuclear industry (Vs=2800 m/s). The number of model predictors is limited to a few measurable parameters: moment magnitude **M**, closest distance to fault rupture plane R_{rup}, average shear-wave velocity in the upper 30 m of the geological profile V_{S30}, and anelastic attenuation factor Q_0. Incorporating anelastic attenuation Q_0 as an input parameter allows adjustments based on the regional crustal properties. The model covers the range of moment magnitudes 4.0<**M**<8.5, rupture distances of 0<R_{rup}<1000 km, S-wave velocities of 450<V_{S30}<2800 m/s in the upper 30 m and frequencies of 0.1<f<100 Hz. Comparisons of the G-16 model with a number of existing CENA GMPEs are shown. In general, the G-16 model compares reasonably well with most of the current models, including the most recent NGA-East model. Estimate of standard error is presented.

Keywords: Ground Motion Prediction Equations; NGA-East; PGA; 5%-damped pseudo spectral acceleration

1. Introduction

This paper presents a new ground motion prediction equations model (G-16) for the Central and Eastern North America (CENA). The model is developed based on the results of the Next Generation Attenuation Relationships for Central and Eastern North-America (NGA-East) multi-disciplinary research project coordinated by the Pacific Earthquake Engineering Research Center (PEER). The goal of the NGA-East project was to develop ground motion attenuation model of an average horizontal component on hard rock sites for the Central and Eastern North America region that reaches into Canada. Under this project, the new NGA-East ground motion database (Goulet et al., [3]) was created.

In contrast to the active tectonic environment in the Western United States (WUS), the new NGA-East strong motion record database for the stable continental environment in the Central and Eastern North America is not sufficient for creating purely empirical ground motion prediction equations (GMPE) covering the range of magnitudes and distances required for seismic hazard assessments. Recorded data collected in the NGA-East database are sparse and cover mostly a limited range of moment magnitudes **M**<6.0 with only three data points with **M**>6 from the 1985 **M**=6.8 Nahanni earthquakes. There are also only a few near-fault recordings which complicate constraining the GMPE even more.

This paper presents an update relative to the G-14 model developed during the NGA-East PEER project, and is called G-16. The updated G-16 model, relative to the previous G-14 model, produces higher high-frequency amplitudes with similar low-frequency amplitudes as a result of a more strict use of the processed data. This GMPE model for the CENA is based on the same modular filter-based approach developed by Graizer and Kalkan for active tectonic environment [1, 2, 4]. The functional forms of the GMPE are derived from filters—each filter represents a particular physical phenomenon affecting the seismic wave radiation from the earthquake source.

The number of predictors used in the model is limited to a few measurable parameters: moment magnitude (**M**), closest distance to fault rupture plane (R_{rup}), average shear-wave velocity in the upper 30 m of the geological profile (V_{S30}), and anelastic attenuation factor (Q_0).

The G-16 model is based on the subset of the recent NGA-East database for the horizontal peak ground acceleration and 5%-damped pseudo-spectral acceleration RotD50 component (Goulet et al., 2014). Fig. 1 demonstrates the subset of 5026 data points from this database with **M**≥3.75 and fault distances of $R_{rup} \leq 1000$ km used to constrain the G-16 model. The average V_{S30} in this subset of all records data is 640 m/s. The dataset includes 48 earthquakes from different regions in the CENA, not distinguishing between the Mid-Continent and Gulf Coast regions. Mid-Continent data dominate the dataset. I did not use data with lower magnitudes since I did not want low-amplitude, non-damaging recordings to dominate the dataset. Additional 2073 recordings from distances $1000<R_{rup}\leq 1500$ km were used for visual comparison with the model predictions.

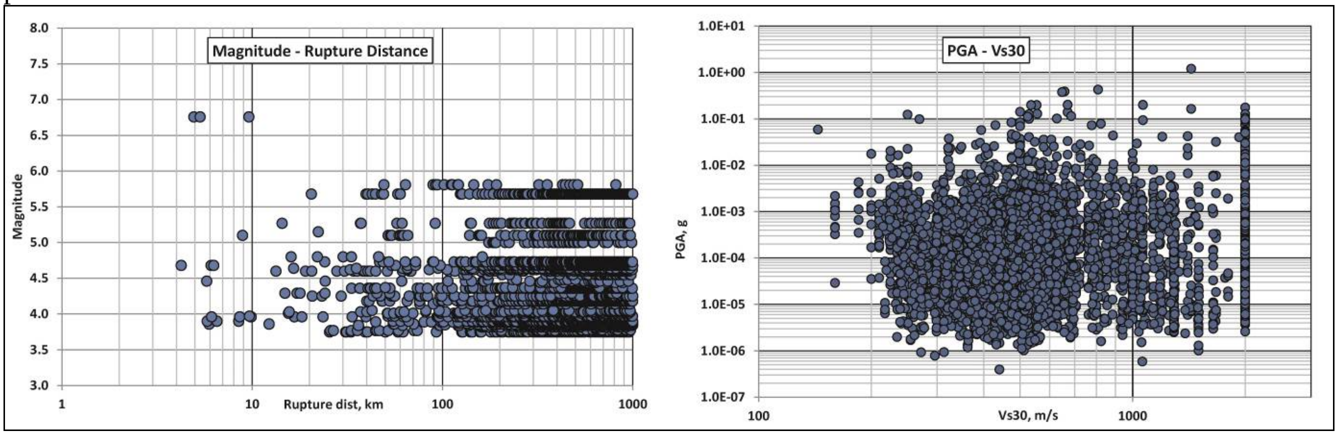

Fig. 1 – Magnitude-distance (left) and PGA-V_{S30} (right) distribution in the subset of database used.

2. PGA Attenuation Model

In this approach (Graizer and Kalkan [1, 2, 4]; Graizer [5]), the GMPE is expressed as a series of filters—each filter represents a certain physical phenomenon affecting the radiation of seismic waves from the earthquake source. In this representation, filters (denoted as G_n in Eq. (1), where n is the filter number) are in multiplication form (cascade of filters). This approach simplifies controlling their relative contributions on resultant ground-motion intensity measures and allows adjustment of a filter if needed.

$$PGA = G_1 \times G_2 \times G_3 \times G_4 \times G_5 \times \varepsilon_Y \tag{1}$$

In Eq. 1, G_n is a function of a set of independent parameters representing moment magnitude, rupture distance, style of faulting, shallow site conditions, basin depth and other parameters affecting the physical process of ground-motion distance attenuation with random error term ε_Y with a mean of zero and a standard deviation σ_Y. The latest Graizer-Kalkan GMPE for PGA was composed of five different filters (Eq. 1) (Graizer and Kalkan [4]). For consistency I am keeping the same number of filters for the G-16 CENA GMPEs (Fig. 2).

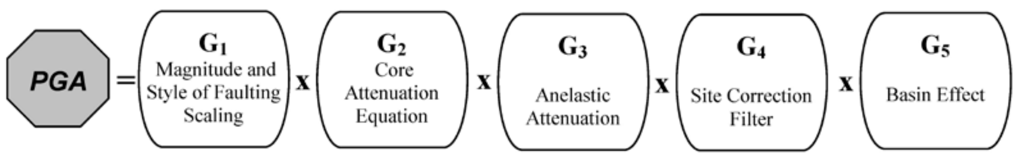

$$ln(PGA) = ln(G_1) + ln(G_2) + ln(G_3) + ln(G_4) + ln(G_5) + \varepsilon_Y$$

Modules

$$ln(G_1) = ln\left([c_1 \arctan(M + c_2) + c_3]\ F\right)$$

$$ln(G_2) = -0.5 ln[(1 - r_2)^2 + 4 D_2^2 r_2]$$

$$\ln(G_3) = -\frac{c_{11} + c_{12} M}{Q_0} R_{rup}$$

$$\ln(G_4)_{PGA} = -0.10805$$

$$\ln(G_5) = 0$$

Where:

$$r_2 = R_{rup} / R_2$$

$$R_2 = c_4 \mathrm{M} + c_5 \quad D_2 = 0.7$$

$$Q_0 = 650 \text{ for CEUS}$$

$$Q_0 = 300 \text{ for Gulf Coast region}$$

Estimator Coefficients

c_1	c_2	c_3	c_4	c_5	c_6	c_7	c_8	c_9
0.40	-6.25	0.55	2.237	-7.542	-0.125	1.19	-6.13	0.60

c_{11}	c_{12}	F	σ
3.9	-0.3445	2.232	0.848

Note: *R_{rup} = Closest fault distance and* **M** *= Moment magnitude*

Fig. 2 - G-16 PGA model for the free-field average horizontal component of ground motion.

2.1 Magnitude Scaling

In my new model, the first filter, G_1 is for magnitude scaling with the same approximation function type as for the WUS [1], except for no dependence on style of fault scaling:

$$A(M, F) = [c_1 \arctan(M + c_2) + c_3]\ F \tag{2}$$

Coefficients c_n and factor F in Equation (2) were originally determined by fitting into median GMPE prepared by EPRI [6] and checked against Pezeshk et al. [7] as part of constructing initial "backbone" model.

The "backbone" model coefficients c_n and factor F are adjusted based on a combination of:

- Ratios of amplitudes of response spectra (RS) of earthquakes with 3.75<**M**<6 from the NGA-East database relative to the NGA-West.
- Average stress-drop ratio between the WUS and CENA. According to published estimates, median stress drop for the intraplate (CENA) earthquakes is 2-3 times higher compared to the interplate (WUS) earthquakes [8, 9].
- Recent NGA-East validated ground motion simulation ratios between **M** 5.0 and higher **M** (Goulet et al., [10]). Comparisons with ground-motion simulations are discussed in more detail later.

Based on the above mentioned results, in the G-16 model, factor F is 2.5 times higher than the same factor for the WUS used in GK-15 model (Graizer and Kalkan [4]). These factors are: F_{WUS}=0.893 and F_{CENA}=2.232.

Similar to the WUS, CENA PGA practically saturates with **M**=8.

2.2 Distance Scaling

The G_2 filter models the distance attenuation of ground-motion and is similar to the frequency response function of a damped single-degree-of-freedom oscillator. This filter is expressed as:

$$G_2(M, R_{rup}) = \frac{1}{\sqrt{\left[1 - (R_{rup}/R_2)\right]^2 + 4D_2^2 (R_{rup}/R_2)}} \tag{3}$$

in which R_2 is the corner distance in the near-source defining the plateau without significant attenuation of ground-motion. This parameter is directly proportional to the moment magnitude of an earthquake; the larger is **M**, the wider is the plateau defined by R_2. Corner distance is proportional to the moment magnitude **M** with the scaling law previously developed for the active tectonic environment [1] (Fig.2):

$$R_2 = c_4 M + c_5 \tag{4}$$

There is an analogy between corner distance R_2 and the corner frequency defined in Brune's model [11] since both are related to the earthquake magnitude. Eqs. (3 and 4) imply that for larger magnitudes, the turning point on the attenuation curve occurs at larger distances. In a way, "flat area near-source ground motion" in my model is similar to the Joyner-Boore distance approach, where all sites within the surface projection of the fault are considered to be at zero distance. I don't expect that the "flat area near-source ground motion", and correspondingly the turning points R_2 are significantly different between stable (CENA) and active (WUS) tectonic environments. Based on the assumption of the similarity of fault dimensions corresponding to certain moment magnitudes, and since there is not enough information to constrain it based on CENA data, in my new models for the CENA, I kept the turning point the same as for the WUS [1]. I assigned parameter D_2=0.7, which is equivalent to no "bump" (increase in amplitude of ground motion at certain distances from the fault also called over saturation) on PGA attenuation with a smooth transition from a plateau to the R^{-1} attenuation (geometrical spreading).

I conducted testing of the slope of attenuation of the response spectra amplitudes at the 9 frequencies between 0.1 and 100 Hz. Average slope of the distance attenuation within the 50-70 km distance from the fault is ~ -1.0 at 7 out of 9 frequencies. For frequencies of 0.5 and 0.2 Hz the slope is ~ -1.3. Taking into account that total attenuation is a combination of geometrical spreading and anelastic attenuation I concluded that classical body-waves geometrical spreading of R^{-1} best fit the data.

2.3 Anelastic Attenuation

The G_3 filter adjusts the distance attenuation rate by including anelastic attenuation given as:

$$G_3(M, R_{rup}, Q) = \exp[(-\frac{c_{11} + c_{12}M}{Q_0})R_{rup}] \tag{5}$$

Eq. (5) is equivalent to $Q=Q_0 f^{1.0}$ where Q_0 is the regional quality-factor for propagation of seismic waves from the source to the site at a frequency of 1 Hz, and c_{11} and c_{12} are coefficients fitted by regression. Eq. (5) changes the PGA attenuation rate after it is plugged into Eq. (1). The value for Q_0 varies regionally and is about 650-1000 for the CENA [12, 13]. Based on my previous tests [4], I concluded that it is reasonable to use a constant $Q=Q_0$ typical for a given region/path (usually that for *Lg* or Coda waves). Pasyanos [13] demonstrated that incorporating laterally variable Q into a GMPE, without even taking into account the effect of V_{S30} improves agreement between empirical data and a model prediction. In my CENA model, I am assuming frequency independent anelastic attenuation. Previous experience with active tectonic environments demonstrated that adjusting Q_0 in our GMPE based on published regional data produces a better attenuation fit than other attenuation models, not having Q_0 as a direct input parameter [4, 14]. I expect that the G-16 model can be adjusted to other stable tectonic regions, for example the Gulf Coast region, by using Q_0 values typical for that region. I assigned Q_0=650 for the main CENA region and Q_0=365 for the Gulf Coast region [15].

To fit the data, I had to assume anelastic attenuation to be magnitude dependent with higher magnitudes producing lower PGA decay. The simplest explanation for this is that larger magnitude events generate a wider spectrum of waves, with longer period waves attenuating slower and creating more converted waves. It is also important to underscore that anelastic attenuation associated with response spectral values are different from that of typical seismological anelastic attenuation of Fourier spectral amplitude. Anelastic attenuation of RS should be higher (Q–values are lower) than the typical seismological one because it also includes damping of the oscillator.

2.4 Site Response Term

The goal of the NGA-East project was to create a set of GMPE models for hard rock conditions. The complexity of that goal is that none of the records in the database were actually recorded at these conditions. Maximum V_{S30} in the database is 2000 m/s, with an average of V_{S30}=640 m/s between all records in my subset. The G_4 filter models ground-motion amplification due to the shallow site conditions (V_{S30}). I developed site correction based on multiple runs of different representative *S*-wave velocity profiles through SHAKE-type equivalent-linear (EQL) programs using time histories and random vibration theory (RVT) approaches [16], and an EQL RVT type code developed at the U.S. Nuclear Regulatory Commission. Site amplification functions are calculated for different V_{S30} relative to hard rock definition used in nuclear industry (Vs=2800 m/s):

$$\begin{gathered} Lin\_Amp = 1 + \frac{k_{Vs30}}{\sqrt{\left[1-(f_{Vs30}/f)\right]^2 + 1.96(f_{Vs30}/f)}} \\ k_{Vs30} = -0.5\ln(V_{S30}/2800) \\ f_{Vs30} = V_{S30}/120 - 1.6 \end{gathered} \tag{6}$$

$$G_4(V_{S30}) = Lin\_Amp(V_{S30}) / Lin\_Amp(V_{VA})$$

where f is frequency. This linear site amplification function covers the range of 450<V_{S30}<2800 m/s, but practically can be applied to all data in the subset of the NGA-East database used in this paper, since data with even lower V_{S30} have very low amplitudes and are not expected to produce non-linearity (Fig. 1, right panel). Developed site correction from V_{S30}=2800 m/s hard rock conditions to V_{S30}=760 m/s (reference site condition used in the development of the U.S. National Hazard Maps) compares well with the frequency-dependent conversion factors used in a number of releases of the U.S. National Hazards Maps [17] including the most recent release of 2014. Similar shapes of site amplification transfer functions were observed in response spectral ratios of recorded earthquake ground motions at downhole geotechnical arrays in California [18]. For example, median high-frequency amplification observed at the Treasure Island downhole array (near San Francisco) from the relatively hard rock (V_S≈2000-2400 m/s) to the alluvial layers (V_S≈380 m/s) was about 1.4 times, increasing to 3.75 times at the surface (V_S≈200 m/s). Eqs. (6) produce similar in shape site amplification functions as linear elastic amplification factors developed for NEHRP site categories A, B, C, D and E, but with lower coefficients of amplification.

I also developed the non-linear portion of the site correction. Non-linearity in this model starts at V_{S30}=450 m/s, and site amplification decreases proportionally to PGA (PSA) starting from accelerations higher than 0.05g (a real effect starts being visible for PGA>0.1g). Non-linear effects are not expected in the current subset of data.

The G_5 filter is for the basin effect, and was developed and calibrated based on California data [4]. This filter is a function of three parameters; these are (1) depth to 1.5 km/sec shear-wave velocity isosurface under the site, denoted as $Z_{1.5}$; (2) distance from the earthquake source; and (3) period (T). Since there is no data to calibrate this filter for CENA, it is set to 1, and does not produce any effect on attenuation in the GMPE version for the CENA.

3. PGA-Based Predictive Model for Spectral Acceleration

Following the approach developed in Graizer and Kalkan [2] for WUS spectral acceleration prediction model, PGA is explicitly integrated as a scaling factor for the spectral shape, which is a continuous function of spectral period (or frequency). Thus, it allows for prediction of SA at any period of interest within the model's range of 0.01 to 10 s or even longer periods (SA at longer periods is not constrained by data, and should be considered to be only an extrapolation). Fig. 3 summarizes this model.

As was shown previously [2, 4], summation of a modified lognormal probability density function with an altered single-degree-of-freedom oscillator transfer function (Fig. 3) eventually provides the desired shape and also enough flexibility to fit into wide range of spectral shapes of real recordings, and their combination results in a working predictive model.

I made a number of modifications to the WUS model to fit the CENA data. For example, in the current G-16 model, spectral slope ζ at long periods is magnitude dependent with slower decay for larger magnitudes for **M**>5.25. The fastest slope is 2.25 for small events with **M**≤5.25, and the slower of 1.5 is for large **M**≥8.0 events. This modification to the spectral slope at long periods is done based on data up to magnitudes ~6.0 and judgement for larger magnitude events.

Based on comparisons of the average RS at different distances from the fault I also observed the same tendency as seen in the WUS: A shift of the peak of response spectra with distance toward longer periods [5]. I did not observe this tendency in the published EPRI [6] ground motion model.

4. G-16 Model Development

As a first step, I created a backbone model based on the EPRI 2013 database and models [6]. At the second step, I adjusted the backbone model based on the residuals using the current NGA-East database [3], and created the new G-16 model.

$$SA(T) = PGA \times \left(SA_{norm}(T/M, R_{rup}) \bullet G_4(V_{S30})\right)$$

$$SA_{norm}(T/M, R_{rup}, V_{S30}) = I(M, R_{rup})\, e^{-\frac{1}{2}\left(\frac{\ln(T)+\mu(M,R_{rup},V_{S30})}{S(M,R_{rup})}\right)^2} + \left[\left(1-\left(T/T_{sp,0}\right)^{\zeta}\right)^2 + 4D_{sp}^2\left(T/T_{sp,0}\right)^{\zeta}\right]^{-1/2}$$

$$\mu(M, R_{rup}) = m_1 R + m_2 M + m_3$$
$$I(M, R_{rup}) = 1.4$$
$$S(M, R_{rup}) = s_1 R_{rup} - (s_2 M + s_3)$$
$$T_{sp,0}(M, R_{rup}, V_{S30}) = t_1 R_{rup} + t_2 M + t_3$$
$$\zeta(M) = a_1 M^2 + a_2 M + a_3$$

R_{rup} = Closest fault distance
M = Moment magnitude

m_1	m_2	m_3	a_1	a_2	a_3	D_{sp}
-0.002	-0.12	3.0	0.0347	-0.5542	3.694	0.75

t_1	t_2	t_3	s_1	s_2	s_3	VA
0.0008	0.16	-0.4875	0.0	0.077	0.3251	640

$$Lin\_Amp = 1 + \frac{k_{Vs30}}{\sqrt{\left[1-\left(f_{Vs30}/f\right)\right]^2 + 1.96\left(f_{Vs30}/f\right)}}$$

$$k_{Vs30} = -0.5\ln(V_{S30}/2800) \quad and \quad f_{Vs30} = V_{S30}/120 - 1.6$$

$$G_4(V_{S30}) = Lin\_Amp(V_{S30}) / Lin\_Amp(V_{VA})$$

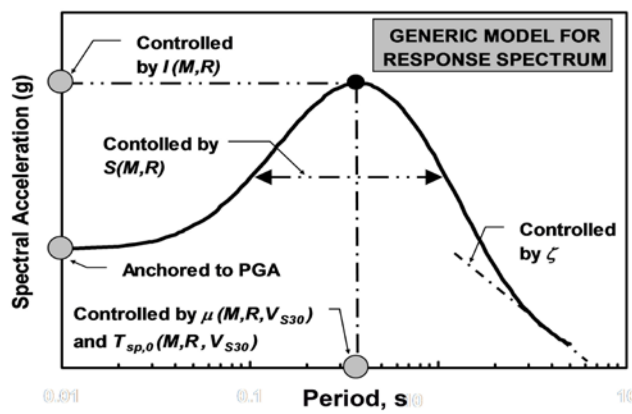

Fig. 3 - PGA-based G-16 model for 5%-damped pseudo spectral acceleration RotD50 component.

Fig.4 demonstrates examples of the spectral acceleration functions for magnitudes 4.5≤**M≤**8.5 at fault distances of 1 and 20 km produced by the G-16 model. As can be seen from these examples, in contrast to the WUS, CENA response spectra flatten at much higher frequencies. In the G-16 model, response spectra flatten completely at a frequency of 250 Hz (0.004 s), and this corresponds to the value of PGA. Differing from the WUS models, PGA is lower than spectral acceleration at a frequency of 100 Hz. PGA and acceleration values at a frequency of 100 Hz should not be used interchangeably for the stable continental environment.

I performed comparisons of the G-16 spectral acceleration functions for the CENA with the GK-15 [4] for the WUS at rupture distances R_{rup} of 5, 20, 100, 200 and 400 km (upper limit for the western model) for V_{S30}=760 m/s. This shear-wave velocity was chosen since it is applicable for both WUS and CENA models, while eastern hard rock velocity is not applicable for the western GMPE models. The high frequency amplitudes of the G-16 spectral acceleration functions are few times higher than those of GK-15, while the low frequency amplitudes are similar at distances of up to about 100 km. Similarities of the low-frequency SA values are expected up to certain distances because of the differences in an anelastic attenuation. At distances more than 200 km predicted low-frequency ground motions in the West are as expected lower because of higher anelastic attenuation (lower Q_0). These comparisons are important since there is no reason to believe that seismic sources in the stable continental region produce different long period motions than those in the active tectonic environment. These results are in agreement with findings of Silva et al. [19], demonstrating based on point-source model that WUS and CENA response spectra have comparable levels for frequencies below 3 Hz with shift of the CENA spectral peak to higher frequencies, and higher PGA values.

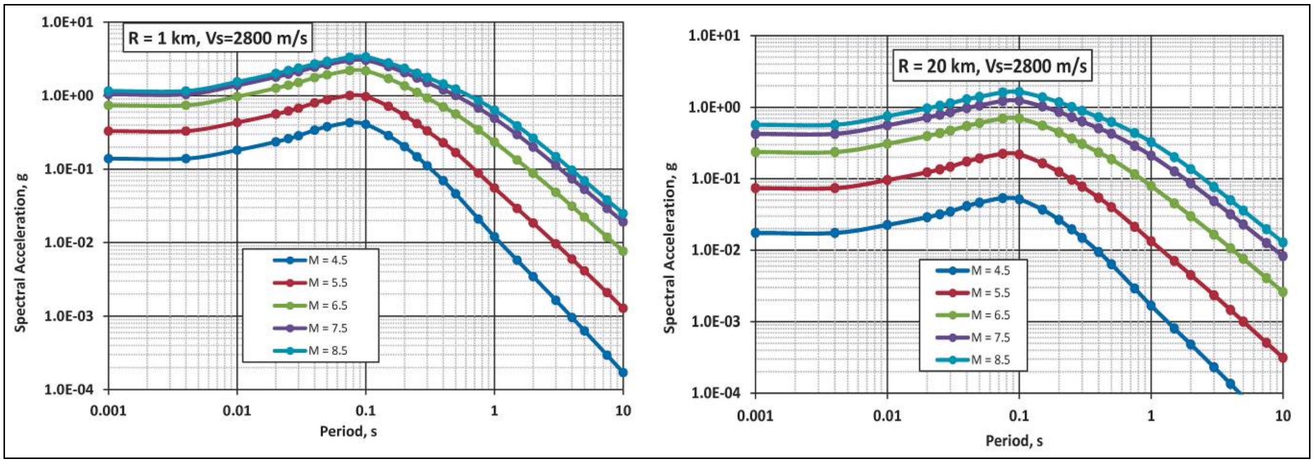

Fig. 4 - Examples of SA functions for 4.5≤**M**≤8.5 at R_{rup} of 1 and 20 km for hard rock conditions produced by the G-16 model.

Fig.5 shows SA magnitude scaling for the frequencies of 10 and 0.5 Hz for hard rock conditions. Similar to the western models, magnitude scaling at different frequencies saturates at large magnitudes.

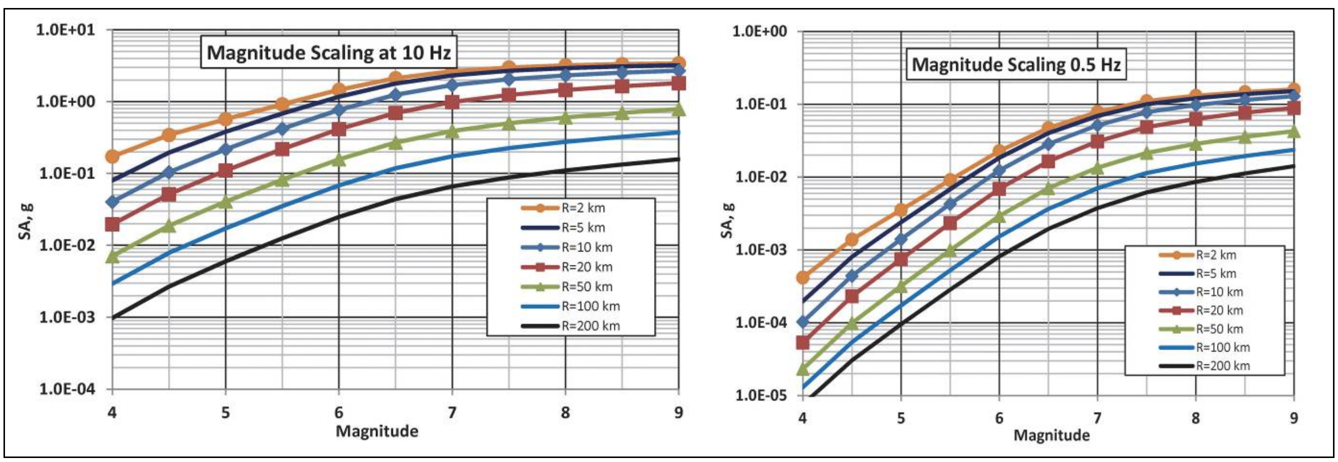

Fig. 5 – G-16 magnitude scaling at spectral accelerations of 10 and 0.5 Hz for hard rock conditions.

The G-16 model was compared to recent ground motion simulations validated during the NGA-East project [10]. These models are: Stochastic Finite-Fault Ground-Motion Simulation Algorithm (EXSIM), Graves and Pitarka (GP) broadband method, and San Diego State University (SD) broadband generation. The model compares well in terms of amplitudes and shapes for frequencies higher than 2 Hz. For lower frequencies, the G-16 model demonstrates similar general behavior, but predicts lower ratios relative to **M**=5.0. The validation exercise report states that for periods above 1 second there is increased bias relative to recordings, and above 3 seconds period there are significant deviations from GMPEs. The high ratios of long-period motions predicted by simulations are not in agreement with NGA-East data.

Fig.6 compares the G-16 model with previously published individual seven models for the CENA for magnitudes 5.5, 6.5 and 7.5 at PGA, and spectral frequencies of 10 Hz and 1 Hz. The G-16 model demonstrates reasonable agreement with the previously published models.

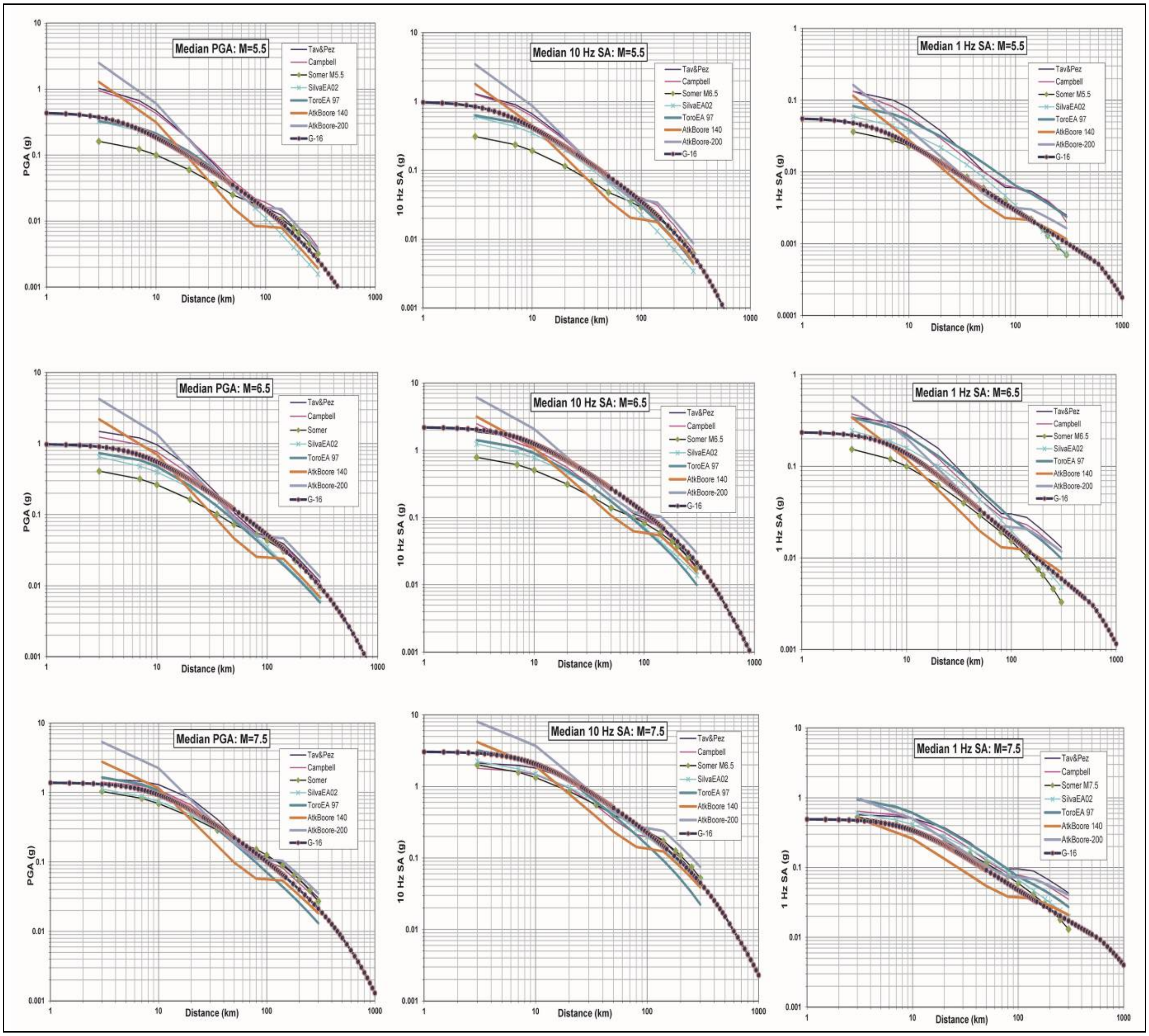

Fig. 6 - Comparison of the G-16 model with the individual seven CENA models for hard rock conditions.

The model was also compared to the EPRI 2013 [6] models for magnitudes **M**=5.0 and **M**=7.5 and all seven frequencies (0.5, 1, 2.5, 5, 10, 25 and 100 Hz) used in the nuclear industry. In general, the G-16 model demonstrates reasonable agreement with the median EPRI 2013 model, and lies within the distribution of the EPRI clusters (Fig.7).

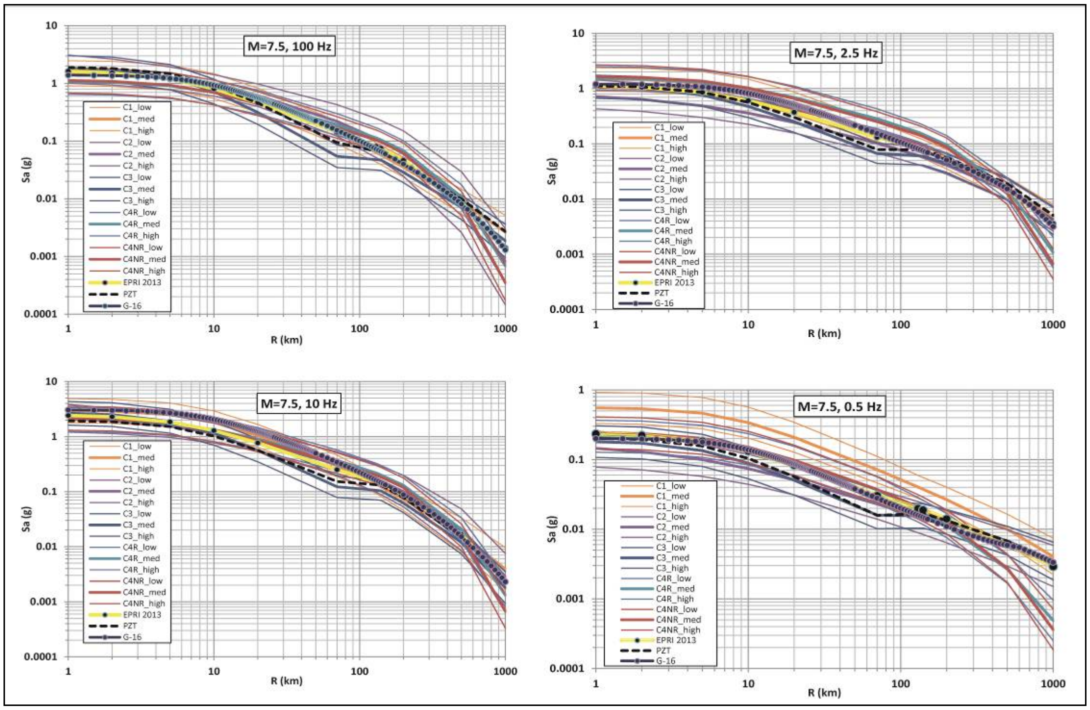

Fig. 7 - G-16 model compared to the median EPRI 2013 model [6] and low, median and high EPRI clusters for **M**=7.5 and hard rock conditions.

5. Residuals and Standard Deviations

Evidently, it is a challenging task to create a GMPE that works in the range of distances from 0 to 1000 km. In the case of the CENA, similar to our approach for the WUS (Graizer and Kalkan [1, 2]) I first attempted to create a model with the coefficients shown in Fig.2 and 3 working at all frequencies, but found out that the residual curves still have trends with over prediction at closer distances and under prediction at large rupture distances. To correct for these trends, I added linear trend corrections at each period of interest.

I calculated the total natural logarithmic standard error (σ) relative to the subset of the recent NGA-East database for magnitudes more than 3.75 and distances up to 800 km. I also made an attempt of splitting total sigma into within-event (ϕ) and between-event (τ) standard deviations.

$$\sigma = \sqrt{\phi^2 + \tau^2} \quad \textbf{(7)}$$

Fig.8 demonstrates smoothed G-16 model standard deviations σ, ϕ and τ curves.

The NGA-East project developed a model for the composite total ergodic magnitude dependent sigma based on the more abundant western database [20]. In average, empirically calculated standard error for the G-16 model is similar to the total composite ergodic sigma estimated by the NGA-East project using NGA-West data. My estimates of the within-event ϕ and between-event τ standard deviations for the G-16 model demonstrate similar behavior as the ones calculated using regression approach and NGA-East data up to the distances of 500 km (Al Atik, [20]: Figs. 4.49 and 4.50). Considering the limitation of the NGA-East database not having large magnitude data and enough near-source recordings, shown G-16 σ, ϕ and τ should be considered as approximations.

Standard deviation for the CENA demonstrates significantly different behavior compared to the WUS. For example, σ in the GK-15 model is constant from PGA until about 0.35 s, and later increases linearly with increasing period. This is a result of significant differences in the NGA-West and NGA-East datasets. The first one has many more reliable data at short periods (< 0.1 s) and a very limited number of reliable long period (> 2

s) data, while the second one has the opposite characteristics: a lot of reliable long-period and very limited number of short-period data. This happens because the NGA-West database is based on recordings of strong-motion instruments, while the NGA-East database is dominated by weak motion velocity recordings.

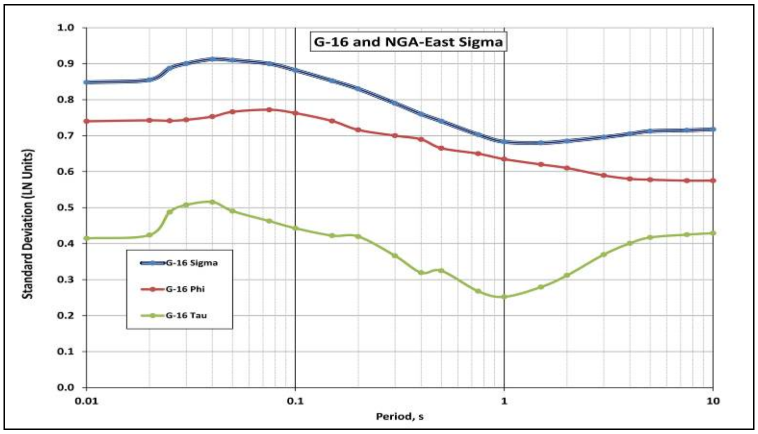

Fig. 8 - G-16 standard deviation (σ), and the within-event (ϕ) and between-event (τ) standard deviations.

6. Results

The new G-16 GMPE model for the CENA is developed following a filter-based approach first introduced by Graizer and Kalkan [1, 2] for the active tectonic environment. The model uses the same set of functions as in the WUS, with the calibration (coefficients) adjusted based on the NGA-East database of September 2014 for the horizontal peak ground acceleration and 5%-damped pseudo spectral acceleration RotD50 component [3].

Comparisons are made of the G-16 model with EPRI 2013 [6] and a number of other published GMPEs. In general, the G-16 model compares reasonably well with most of the current models, including the most recent NGA-East model.

Incorporating anelastic attenuation Q_0 as an input parameter allows adjustments based on the regional crustal properties. The G-16 model can be adjusted to other stable tectonic regions, for example the Gulf Coast region, by using $Q_0 \approx 350$ typical for that region, instead of $Q_0 \approx 650$ typical for the main CENA region [15].

The model covers the range of moment magnitudes of $4.0 \leq \mathbf{M} \leq 8.5$, distances of $0 \leq R_{rup} \leq 1000$ km, S-wave velocities of $450 \leq V_{S30} \leq 2800$ m/s and period range of 0.01 to 10 s. The model is actually extrapolated to produce reasonable results for distances up to 1500 km by the request of the leaders of the NGA-East project, since seismic hazard runs sometimes require distances more than 1000 km.

The Graizer-16 (G-16) ground motion prediction equations for spectral acceleration are available from the author in MatLab format.

6. Acknowledgements

I am grateful to Scott Stovall, Clifford Munson, Dogan Seber, Shahram Pezeshk, Martin Chapman, Nicolas Kuehn and Linda Al Atik for critical reviews, valuable comments and suggestions that helped improve the quality of the model.

7. Disclaimer

Any opinions, findings and conclusions expressed in this paper are those of the author and do not necessarily reflect the views of the U.S. Nuclear Regulatory Commission.

8. References

[1] Graizer, V. and Kalkan, E. (2007). Ground-motion attenuation model for peak horizontal acceleration from shallow crustal earthquakes, *Earthquake Spectra*, **23** (3), 585-613.

[2] Graizer, V. and Kalkan, E. (2009). Prediction of response spectral acceleration ordinates based on PGA attenuation, *Earthquake Spectra*, **25** (1), 39-69.

[3] Goulet, C., Ancheta, T., Cramer, C., Mueller, C. and J. Rubenstein (2014). NGA-East 5%-Damped RotD50 Flatfile Release, v.20140912.

[4] Graizer, V. and Kalkan, E. (2016). Summary of the GK15 Ground-Motion Prediction Equations for Horizontal PGA and 5% Damped PSA from Shallow Crustal Continental Earthquakes**.** *Bull. Seism. Soc. Am*., **106**, 687-707.

[5] Graizer, V. (2015). Ground-Motion Prediction Equations for the Central and Eastern United States. In: *NGA-East: Median Ground-Motion Models for the Central and Eastern North America Region. Pacific Earthquake Engineering Research Center (PEER) Report No. 2015/04*, 213-249.

[6] EPRI (2004, 2006), (2013). Ground-Motion Model (GMM) Review Project. 3002000717. *Final Report. June 2013. Electric Power Research Institute.* 3420 Hillview Avenue, Palo Alto, CA 94304. Appendix A. Description of project database.

[7] Pezeshk, S., Zandieh, A., and Tavakoli, B. (2011). Hybrid empirical ground-motion prediction equations for Eastern North America using NGA models and updated seismological parameters, *Bull. Seism. Soc. Am*., **101**, 1859-1870.

[8] Atkinson G.M., Wald D.J. (2007). “Did you feel it?” intensity data: a surprisingly good measure of earthquake ground motion, *Seismol. Res. Lett.*, **78**: 362–368.

[9] Allmann, B. P., and P. M. Shearer (2009). Global variations of stress drop for moderate to large earthquakes. *Journal Geophys. Res*., **114**, B01310, 1-22.

[10] Goulet, C. A., N. A. Abrahamson, P. G. Somerville, and K. E. Wooddell (2015). The SCEC broadband platform validation exercise: Methodology for code validation in the context of seismic hazard analyses, *Seismol. Res. Lett*. **86**, 17-26.

[11] Brune, J. (1970). Tectonic stress and the spectra of seismic shear waves from earthquakes. *J. Geophys. Res.*, **75**, 4997-5009.

[12] Erickson, D., D. E. McNamara, and H. M. Benz (2004). Frequency-dependent Lg Q within the continental United States*. Bull. Seism. Soc. Am*., **94**, 1630-1643.

[13] Pasyanos, M. E. (2013). A Lithospheric attenuation model of North America, *Bull. Seismol. Soc. Am*. **103**, 3321-3333.

[14] Baltay, A.S., and J. Boatwright (2015). Ground-Motion Observations of the 2014 South Napa earthquake. *Res. Lett*. **86**, 355-360.

[15] Chapman, M., and Conn, A. (2016). A model for Lg propagation in the Gulf Coastal Plain of the Southern United States, *Bull. Seismol. Soc. Am*. **106**, 349-363.

[16] Kottke, A. R., and E. M. Rathje (2008). Technical manual for Strata, Report 2008/10, *Pacific Earthquake Engineering Research (PEER) Center*, Berkeley, California, 95 p.

[17] Frankel, A., Mueller, C., Barnhard, T., Perkins, D, Leyendecker, E.V., Dickman, N., Hanson, S., and Hopper, M. (1996). National seismic hazard maps—Documentation June 1996: *U.S. Geological Survey Open-File Report* 96-532, 110 p.

[18] Graizer, V. (2014). Comment on “Comparison of Time Series and Random-Vibration Theory Site-Response Methods” by Albert R. Kottke and Ellen M. Rathje. *Bull. Seism. Soc. Am*., **104**, 540-546.

[19] Silva, W. J., R.R. Youngs, and I.M. Idriss (2001). Development of design response spectral shapes for Central and Eastern U.S. (CEUS) and Western U.S. (WUS) rock site conditions. In: *Proc. of the OECE-NEA (Organization for Economic Coordination and Development of the Nuclear Energy Agency) Workshop on Engineering Characterization of Seismic Input, Nov., 15-17, 1999 NEA/CSNI/R (2000)2,* **1**, 185-268.

[20] Al Atik, L. (2015). NGA-East: Ground-Motion Standard Deviation Models for Central and Eastern North America. Pacific Earthquake Engineering Research (PEER) Center. Report 2015/07, 182 p.